IEEE Access
Multidisciplinary ⁝ Rapid Review ⁝ Open Access Journal

Received 3 May 2023, accepted 5 June 2023, date of publication 14 June 2023, date of current version 19 June 2023.

Digital Object Identifier 10.1109/ACCESS.2023.3286022

RESEARCH ARTICLE

Observer-Based Model-Free Adaptive Sliding Mode Predictive Control

BING REN[1,2] AND GUANGQING BAO[3]

[1]School of Automation and Electrical Engineering, Lanzhou Jiaotong University, Lanzhou 730070, China
[2]College of Electrical and Information Engineering, Lanzhou University of Technology, Lanzhou 730050, China
[3]School of Electronics and Information Engineering, Southwest Petroleum University, Chengdu 610500, China

Corresponding author: Bing Ren (ice84_03@163.com)

This work was supported in part by the National Natural Science Foundation of China under Grant 51967012, in part by the Key Research and Development Program of Gansu Province under Grant 20YF8GA055, in part by the Natural Science Foundation of Gansu Province under Grant 22JR5RA359, and in part by the Youth Foundation of Lanzhou Jiaotong University under Grant 2019034.

ABSTRACT This paper proposes a new observer-based model-free adaptive sliding mode predictive control method (MFASPC) for discrete-time nonlinear systems. This scheme first equates the discrete-time nonlinear system to a linear form using a data-driven compact form dynamic linearization (CFDL) technique, establishes a data model consisting of only the pseudo partial derivatives (PPD), input data and output data, designs adaptive observers to achieve the estimation of the unknown PPD. The controller design part uses integral sliding mode control (SMC) to ensure the system's robustness. In contrast, with its constraint characteristics, the model predictive control (MPC) replaces the traditional switching control of SMC. The closed-loop control quantities are obtained by solving a rolling optimization problem in the finite time domain to provide dynamic optimal control action. The theoretical derivation of the Lyapunov function is used to demonstrate the system's stability. In order to verify the effectiveness of the proposed algorithm, numerical simulations and Photovoltaic power generation system simulation experiments are conducted, respectively, and the results show that the proposed control algorithm has a very reliable tracking capability and control accuracy.

INDEX TERMS Adaptive observer, model free, sliding mode predictive control, rolling optimization, data-driven.

I. INTRODUCTION

In recent years, adaptive control techniques for nonlinear systems have attracted a large number of scholars and much effort has been devoted to them [1], [2], [3]. However, most methods require dynamical or mechanistic analysis of the control system to obtain an accurate mathematical model first, and there are inevitably approximation links throughout the process [4]. In contrast, the ignored unmodeled dynamics part may be a potential factor that makes the closed-loop system unstable and reduces the controller performance.

Model-free adaptive control (MFAC) is a data-driven control method for discrete-time nonlinear systems to improve modeling difficulties [5], and its most important features compared to other data-driven control methods are the equivalent dynamic linearization process and the introduction of virtual parameters (PPD). MFAC uses the input and output data of the system to update the virtual parameters online dynamically, thus establishing an equivalent data model, both the PPD and the data model, which depend merely on the data and are unrelated to the structural information of the system, thus thoroughly characterizing the nonlinear and uncertain features of the system [6]. It has been widely used in the past few years, such as urban traffic control, heading control, zero-sum game control, flexible joint control, etc. [7], [8], [9], [10].

As the research progresses, to further solve the uncertainty problem of the control system and ensure robust performance in control, some scholars bring the SMC into the MFAC algorithm to carry out the research, which produces the model-free adaptive sliding mode control (MFASC) scheme.

The associate editor coordinating the review of this manuscript and approving it for publication was Haibin Sun.

This work is licensed under a Creative Commons Attribution-NonCommercial-NoDerivatives 4.0 License.
For more information, see https://creativecommons.org/licenses/by-nc-nd/4.0/

Among them, the sliding phase of the SMC law ensures the excellent stability performance of the system, and the arrival phase determines the system's dynamic performance. For example, [11] implemented model-free adaptive sliding mode control for an autonomous four-wheeled mobile vehicle parking system using vehicle body angle and steering angle data; [12] proposed a new enhanced model-free discrete-time adaptive terminal sliding mode control for solid oxide fuel cell system with input constraints, aiming to regulate the output voltage under load perturbations; [13], [14], and [15] considers the tracking error constraint and introduces a predetermined model-free adaptive integral sliding mode control based on the performance idea, which makes the tracking error converge to a predefined neighborhood; [16] combines MFAC with discrete-time SMC with exponential arrival law and applies it to a multi-degree-of-freedom robot system, where the control process only uses the measured input torque and output velocity of the exoskeleton; the same system, [17] designed an adaptive sliding mode compensator to select a non-singular terminal sliding surface to achieve fast convergence and improve the tracking performance; [18] takes the input saturation problem as the entry point, uses bounded features to overcome the chaotic behavior and achieves model-free adaptive sliding mode control for chaotic fractional-order systems; [19] introduces a sliding-mode-based auxiliary controller, which uses only attitude angle and attitude angular velocity information to improve the model-free adaptive control tracking performance of the combined spacecraft; [20] and [21] applied the model-free adaptive sliding mode control algorithm to a multi-input multi-output systems. However, most of the MFASC algorithms do not consider the optimality problem. The arrival phase that determines the system's dynamic performance still needs improvement and optimization.

MPC is typically characterized by rolling optimization in the predictive time domain, allowing improved dynamic performance in the arrival phase and explicit and active handling of input and state constraints. Considering this advantage, the combination with the SMC that solves for the optimal sliding mode state at each sampling moment makes the sliding mode predictive control method both robust and optimal. [22] designed an integral digital terminal sliding mode predictive control scheme dedicated to precision motion control and experimentally confirmed good tracking accuracy; [23] proposed a continuous control set sliding mode predictive velocity control method to develop a discrete-time integral sliding mode predictive observer to achieve the prediction of the reference velocity and feedforward to a predefined fast terminal sliding-mode-based cost function to achieve one-step prediction of the reference velocity. [24] investigates discrete-time underdriven sliding manifolds and sliding mode prediction equations, and simulations verify more stable and faster tension control. Reference [25] develops robust sliding-mode nonlinear predictive controllers by cascading and smooth sliding-mode controllers to integrate human intent tracking and safety assurance objectives into the optimization problem with robust desired speed tracking. Using quasi-sliding mode bandwidth and good constraint handling capability, [26] is used for accurate motion control with cross-coupled lag nonlinearity. The above studies show that the sliding mode predictive control can provide optimal control actions for the more accurate performance of nonlinear systems. However, the above sliding mode predictive controllers are built based on a piezoelectric-driven motion system, surface-mounted permanent-magnet synchronous motor, space-tethered satellite system, brain-controlled robots, and parallel micropositioning piezo stage, all of which have precise mathematical models and system parameters. When faced with systems that do not or cannot have precise information, [27] improves the robustness of the predictive control system based on an ultra-local model without using parameters and uncertain variables, but the modeling process is relatively computationally complex; [28] combines discrete-time terminal sliding mode predictive control with MFAC method, which simplifies the modeling process, but the signal oscillation phenomenon in the sliding mode switching phase is serious; [29] investigated the tracking problem of multi-intelligent body systems in network systems, combining three methods of MFAC, proportional SMC, and MPC. However, the predictive control structure of this algorithm is not used to optimize control law but for compensate time delays.

Based on the above analysis, this paper proposes an observer-based model-free adaptive sliding mode predictive control method for discrete-time nonlinear systems, which uses an adaptive observer to design a pseudo partial derivative estimation algorithm and establish a tight-format equivalent data model. Compared with other studies, the method proposed in this paper is based on constraints and optimized performance, attenuating the jitter phenomenon in the arrival phase and reducing the steady-state error in the sliding mode phase. The stability analysis of the system is carried out by the Lyapunov method instead of the compression mapping principle commonly used in model-free adaptive control theory. The main contributions include: 1) the switching control in traditional sliding mode control is replaced by rolling optimal control for each sampling period, which avoids frequent oscillations of the output signal near the sliding mode surface, optimizes the control trajectory, and improves the accuracy of the control. 2) the input and input incremental constraint problems are incorporated into the cost function design to exploit the constraint handling capability of the model predictive control, which is described in the literature [28] is not considered; 3) the proposed discrete integral sliding mode predictive control relies only on the system input and output and the corresponding incremental data, not on specific structures and parameters, and has flexible portability.

The remaining parts of the paper are organized as follows. Section II proposes an observer-based PPD estimation algorithm and compact form data model of a discrete-time nonlinear system. The design procedure of the MFASPC algorithm-based data model and corresponding stability analysis are detailed in Section III. In Section IV, Simulation results are shown for the proposed schemes. Section V summarizes this paper.

II. PROBLEM FORMULATION

A. SYSTEM DESCRIPTION

Consider the SISO discrete-time nonlinear system as follows:

$$y(k+1)=f(y(k),y(k-1),\cdots,y(k-w_y),\\ u(k),u(k-1),\cdots,u(k-w_u)) \tag{1}$$

where $y(k)$ and $u(k)$ are the output and input of the system at the moment of sampling time k, respectively, $f(\cdot)$ is the unknown nonlinear function, and w_y and w_u are the unknown orders of the output and input of the system, respectively.

For the systems(1), the following two assumptions should be given first.

Assumption 1: The unknown nonlinear function $f(\cdot)$ is derivable and continuous at any time concerning control input.

Assumption 2: The nonlinear systems satisfy Lipschitz condition. Namely, there is a constant ξ_ϕ such that $\Delta y(k+1) \leq \xi_\phi \Delta u(k)$. where $\Delta y(k+1) = y(k+1) - y(k)$ indicates output increments, $\Delta u(k) = u(k) - u(k-1)$ means input increment.

Remark 1: Assumption 1 is general for controller design. Assumption 2 can be said to be an embodiment of the law of conservation of energy. The amount of control input and input increment determine the amount of output and output increment. If the input change rate of $\Delta u(k)$ for two consecutive work points is too large, the stability of system will quickly deteriorate. This assumption will also make the theoretical analysis more suitable for practical applications, such as the three-tank [5] and temperature control system [13].

According to the dynamic linearization principle based on PPD, the compact form data model of the system (1) when the input increment $\Delta u(k) \neq 0$ can be expressed as:

$$\Delta y(k+1) = \phi(k)\Delta u(k) \tag{2}$$

where $\phi(k)$ is called the PPD, which represents the "virtual input increment gain" at the moment k.

Remark 2: $\phi(k)$ is not a parameter with a definite value. However, it consists of the median of the partial derivatives of the unknown nonlinear function $f(\cdot)$ concerning the control input at a point on the interval at k moments together with a nonlinear residual term with complex dynamic properties. Its size depends only on the nonlinear system's output increment and input increment and is bounded for any moment, and there exists $|\phi(k)| \leq \xi_\phi$.

B. PPD ESTIMATION ALGORITHM BASED ON ADAPTIVE OBSERVER

The compact form data model constantly requires input and output data from the current and historical moments to update and identify $\phi(k)$ of the current moment, which necessitates the design of an adaptive algorithm to estimate $\phi(k)$, introducing the observer structure.

$$\hat{y}_s(k+1) = \hat{y}_s(k) + \hat{\phi}(k)\Delta u(k) + K_s e_s(k) \tag{3}$$

where $\hat{y}_s(k)$ refers to the system output estimation value at k moment, $\hat{\phi}(k)$ describes the system PPD estimation value at k moments, $e_s(k) = y(k) - \hat{y}_s(k)$ is the output estimation error, and K_s is the output estimation error gain satisfying $0 < K_s < 1$. Therefore, the dynamic of output estimation error $e_s(k+1)$ can be written as:

$$e_s(k+1) = \Delta u(k)\bar{\phi}(k) + (1-K_s)e_s(k) \tag{4}$$

where $\bar{\phi}(k) = \phi(k) - \hat{\phi}(k)$ represents the PPD estimation error. According to the structure of the observer (3), the following algorithm can be used for the estimation of the PPD:

$$\hat{\phi}(k+1) = \hat{\phi}(k) + \frac{2\Delta u(k)}{|\Delta u(k)|^2 + \chi}(e_s(k+1) - (1\\ - K_s)e_s(k)) \tag{5}$$

where χ denotes the penalty factor and $\chi > 0$. $e_s(k+1)$ is the output estimation error at future moments, which cannot be used as known data in (5), and the two-step delayed uncertain parameter estimation algorithm is used to estimate, using the output estimation error values at the moment k and previous moments, the following:

$$\hat{e}_s(k+1) = 2e_s(k) - e_s(k-1) \tag{6}$$

Substituting (5) yields the observer-based PPD estimation algorithm as:

$$\hat{\phi}(k+1) = \hat{\phi}(k) + \frac{2\Delta u(k)}{|\Delta u(k)|^2 + \chi}((1+K_s)e_s(k)\\ - e_s(k-1))\\ \hat{\phi}(k) = \hat{\phi}(1), if\, |\hat{\phi}(k)| \leq \varsigma or |\Delta u(k-1)| \leq \varsigma \tag{7}$$

where ς is a remarkably minor positive constant, the non-negative constant $\hat{\phi}(1)$ is the initial value for $\hat{\phi}(k)$. The purpose of resetting $\hat{\phi}(k)$ is to stop it from falling into a local minimum, which helps to improve the control. Meanwhile, the dynamic characteristics of the system output are expressed as follows:

$$y(k+1) = \hat{y}_s(k) + \hat{\phi}(k)\Delta u(k) + (2+K_s)e_s(k)\\ - e_s(k-1) \tag{8}$$

The control objective of this paper is to propose a data-driven model-free adaptive sliding mode predictive control method based on sliding mode predictive control, using the PPD estimated by the adaptive observer and the output dynamic characteristics to achieve accurate tracking control of the system for known signal trajectories.

III. CONTROLLER DESIGN AND STABILITY ANALYSIS

In this section, an observer-based model-free adaptive sliding mode predictive controller is proposed to predict the sliding mode function in the finite time domain by invoking the rolling optimization function of MPC. The optimal output control replaces the traditional switching control, which is jointly equilibrium control, to commonly compose a new control input, making the sliding mode converge to the equilibrium state quickly and smoothly.

A. INTEGRAL SLIDING MODE CONTROL

Select the sliding surface with the integral term:

$$s(k) = e^*(k) + \lambda \sum_{i=1}^{k} Te^*(i) \tag{9}$$

where $\lambda > 0$ is the integral term coefficient, T is the sampling time interval, and $e^*(k)$ is the tracking error, which is the result of the difference between the given desired output $\tilde{y}(k)$ and the actual output $y(k)$, expressed as $e^*(k) = \tilde{y}(k) - y(k)$, thus the dynamic characteristics of the sliding mode surface can be deduced as:

$$s(k+1) = e^*(k+1) + \lambda \sum_{i=1}^{k+1} Te^*(i) \tag{10}$$

$$\begin{aligned}\Delta u_{eq}(k) = {} & \frac{\hat{\phi}(k)}{\hat{\phi}^2(k)+\sigma}(\tilde{y}(k+1) - \hat{y}_s(k) - (2 \\ & + K_s)e_s(k) + e_s(k-1) - \frac{e^*(k)}{1+\lambda T})\end{aligned} \tag{11}$$

where $\Delta u_{eq}(k)$ stands for equivalent control law and $\sigma > 0$.

The switching control acts on the arrival phase and consists of the output $\Delta u_p(k)$ of the predictive controller, i.e., $\Delta u_{sw}(k) = \Delta u_p(k)$, so that the total control action is expressed as: The equivalent control acts on the sliding phase of the SMC, and according to the relation $\Delta s(k+1) = s(k+1) - s(k) = 0$ satisfied on the sliding mode surface, it is possible to find the corresponding equivalent control.

$$\Delta u(k) = \Delta u_{eq}(k) + \Delta u_p(k) \tag{12}$$

where $\Delta u(k)$ is the sliding mode predictive controller output.

Substituting (11), (12) into (10), the sliding mode surface state dynamics can be expressed as:

$$\begin{aligned}s(k+1) = {} & (1+\lambda T)(\tilde{y}(k+1) - \hat{y}_s(k) - (2+K_s)e_s(k) \\ & + e_s(k-1) - \Delta u_p(k)\hat{\phi}(k) - \frac{\hat{\phi}^2(k)}{\hat{\phi}^2(k)+\sigma} \\ & \times (\tilde{y}(k+1) - \hat{y}_s(k) - (2+K_s)e_s(k) \\ & + e_s(k-1) - \frac{e^*(k)}{1+\lambda T})) + s(k) - e^*(k) \\ = {} & s(k) - (1+\lambda T)\hat{\phi}(k)\Delta u_p(k) + \frac{(1+\lambda T)}{\hat{\phi}^2(k)+\sigma} \\ & \times \sigma j(k)\end{aligned} \tag{13}$$

where j(k) denotes the error disturbance term, it is defined as:

$$\begin{aligned}j(k) = {} & \tilde{y}(k+1) - \frac{\tilde{y}(k)}{1+\lambda T} - \frac{\lambda T \hat{y}_s(k)}{1+\lambda T} - (2+K_s \\ & - \frac{1}{1+\lambda T})e_s(k) + e_s(k-1)\end{aligned}$$

B. SLIDING MODE PREDICTIVE CONTROL

Here, the idea of predictive control is introduced to predict the future sliding surface state, and (13) is regarded as the first step prediction of the sliding surface, then the future Nth step prediction of the sliding surface state is:

$$\begin{aligned}s(k+N) = {} & s(k) - (1+\lambda T)(\hat{\phi}(k)\Delta u_p(k) + \hat{\phi}(k+1) \\ & \times \Delta u_p(k+1) + \ldots + \hat{\phi}(k+N-1) \\ & \times \Delta u_p(k+N-1)) + (1+\lambda T) \\ & \times (\frac{\sigma j(k)}{\hat{\phi}^2(k)+\sigma} + \frac{\sigma j(k+1)}{\hat{\phi}^2(k+1)+\sigma} + \ldots \\ & + \frac{\sigma j(k+N-1)}{\hat{\phi}^2(k+N-1)+\sigma})\end{aligned} \tag{14}$$

From (13) and (14), define the predictive control function:

$$s^a(k) = \Lambda s(k) - \Theta \Delta u^a(k-1) + \Upsilon J(k-1) \tag{15}$$

where the vector expressions of $s^a(k)$ and $\Delta u^a(k-1)$ take the form:

$$s^a(k) = \left[s(k+1)\ s(k+2)\ \cdots\ s(k+N)\right]^T$$

$$\Delta u^a(k-1) = \begin{bmatrix}\Delta u_p(k) \\ \Delta u_p(k+1) \\ \vdots \\ \Delta u_p(k+N-1)\end{bmatrix}$$

$$J(k-1) = \left[j(k)\ j(k+1)\ \cdots\ j(k+N-1)\right]^T$$

where Λ, Θ, and Υ are defined as coefficients of each component $s(k)$, $\Delta u^a(k-1)$, and $J(k-1)$ of the predictive control function $s^a(k)$.

Λ denotes the N-dimensional column vector with all elements are 1, Θ is a lower triangular matrix consisting of PPD estimates at each moment, which directly reflects the causality of the system in time, i.e., the input at the last moment has no effect on the output of the sliding mode state at the former moment, and the sliding mode state at the past moment depends only on the control input at the last moment and is independent of the control input at the future moment, in the following format:

$$\Theta = (1+\lambda T)\begin{bmatrix}\hat{\phi}(k) & 0 & \ldots & 0 \\ \hat{\phi}(k) & \hat{\phi}(k+1) & \ldots & 0 \\ \vdots & \vdots & \ddots & \vdots \\ \hat{\phi}(k) & \hat{\phi}(k+1) & \ldots & \hat{\phi}(k+N-1)\end{bmatrix}$$

Similarly, Υ has the lower triangular matrix format:

$$\Upsilon = \begin{bmatrix} \frac{\sigma(1+\lambda T)}{\hat{\phi}^2(k)+\sigma} & 0 & \cdots & 0 \\ \frac{\sigma(1+\lambda T)}{\hat{\phi}^2(k)+\sigma} & \frac{\sigma(1+\lambda T)}{\hat{\phi}^2(k+1)+\sigma} & \cdots & 0 \\ \vdots & \vdots & \ddots & \vdots \\ \frac{\sigma(1+\lambda T)}{\hat{\phi}^2(k)+\sigma} & \frac{\sigma(1+\lambda T)}{\hat{\phi}^2(k+1)+\sigma} & \cdots & \frac{\sigma(1+\lambda T)}{\hat{\phi}^2(k+N-1)+\sigma} \end{bmatrix}$$

Assuming that the prediction time domain and the control time domain are the same, define a cost function for the minimization operation using $s^a(k)$ and $u^a(k-1)$ from the prediction function (15):

$$\begin{aligned} F =& s^a(k)^T s^a(k) + \Delta u^a(k-1)^T R_u \Delta u^a(k-1) \\ & s.t. \quad \Delta u_{min} \leq \Delta u_p(k) \leq \Delta u_{max} \\ & u_{min} \leq u_p(k) \leq u_{max} \end{aligned} \tag{16}$$

where R_u is the diagonal matrix to constrain the control action $\Delta u^a(k-1)$, and u_{max}, u_{min}, Δu_{max}, and Δu_{min} denote the upper and lower bounds of the control action and its incremental change, respectively. The MFASPC problem can be formulated as an optimization problem in which the input signal is determined in N steps to make s(k) converge to the sliding surface by considering the control constraints.

Expressing the constraints in vector form, we have:

$$\begin{aligned} \Gamma u^a(k-2) + \Gamma_\Delta \Delta u^a(k-1) &\leq u^a_{max} \\ -(\Gamma u^a(k-2) + \Gamma_\Delta \Delta u^a(k-1)) &\leq -u^a_{min} \\ \Delta u^a(k-1) &\leq \Delta u^a_{max} \\ -\Delta u^a(k-1) &\leq -\Delta u^a_{min} \end{aligned}$$

where u^a_{max}, u^a_{min}, Δu^a_{max} and Δu^a_{min} are column vectors with all elements of u_{max}, u^a_{min}, Δu_{max} and Δu^a_{min}, respectively. The coefficient Γ denotes the N-dimensional column vector with all elements are 1, and the coefficients Γ_Δ denote the lower triangular matrix consisting of unit matrices. It can be expressed as follows:

$$\Pi \Delta u^a(k-1) \leq \Omega \tag{17}$$

where the coefficients of $\Delta u^a(k-1)$ are:

$$\Pi = \begin{bmatrix} \Gamma_\Delta \\ -\Gamma_\Delta \\ I \\ -I \end{bmatrix} \quad \Omega = \begin{bmatrix} -\Gamma u^a(k-1) + u^a_{max} \\ \Gamma u^a(k-1) - u^a_{min} \\ \Delta u_{max} \\ -\Delta u^a_{min} \end{bmatrix}$$

The predictive control aims to find the optimal control vector $\Delta u_p(k)$ under certain constraints.

$$\begin{aligned} \min_{\Delta u_{pc}(k|k),\ldots,\Delta u_{pc}(k+N-1|k)} F(k) =& \sum_{m=1}^{N} s(k+m|k)^2 \\ &+ \mu \sum_{m=1}^{N} \Delta u^2_{pc}(k+m-1|k) \end{aligned} \tag{18}$$

For minimizing the objective function with constraints, the Lagrangian expression is set as:

$$\begin{aligned} minF =& s^a(k)^T s^a(k) + \Delta u^a(k-1)^T R_u \\ & \times \Delta u^a(k-1) + \mu^T (\Pi \Delta u^a(k-1) - \Omega) \end{aligned} \tag{19}$$

where μ is the Lagrangian multiplier, it is observed that subject to the constraint (17), (18) has the same result as the cost function.

Since the future disturbance value J(k-1) and the PPD matrix Θ are unknown, $j(k)$ and $\hat{\phi}(k)$ are always chosen to estimate the unknown part after k moment:

$$\hat{J}(k-1) = \left[j(k)\ j(k) \cdots j(k)\right]^T$$

$$\hat{\Theta}(k) = (1+\lambda T) \begin{bmatrix} \hat{\phi}(k) & 0 & \ldots & 0 \\ \hat{\phi}(k) & \hat{\phi}(k) & \ldots & 0 \\ \vdots & \vdots & \ddots & \vdots \\ \hat{\phi}(k) & \hat{\phi}(k) & \ldots & \hat{\phi}(k) \end{bmatrix}$$

For obtaining the extreme value solution in the prediction time domain, from the first derivative of the cost function (16) for the vectors $\Delta u_p(k)$, then the optimal control problems in the prediction range are:

$$\begin{aligned} \Delta u^*_p(k) =& -(\Gamma^T_\Delta \hat{\Theta}^T \hat{\Theta} \Gamma_\Delta + R_u)^{-1} (\Pi^T \mu^* + \Gamma^T_\Delta \\ & \times (-\hat{\Theta})^T (s(k) + \Upsilon \hat{J}(k-1)) \end{aligned} \tag{20}$$

where μ^* is the optimal value of the Lagrange multiplier, which can be given by the partial derivative of (16) relative to the vector μ.

Choose the first element of $\Delta u^*_p(k)$.

$$\begin{aligned} \Delta u_p(k) =& -\delta(\Gamma^T_\Delta \hat{\Theta}^T \hat{\Theta} \Gamma_\Delta + R_u)^{-1} (\Pi^T \mu^* \\ & + \Gamma^T_\Delta (-\hat{\Theta})^T (s(k) + \Upsilon \hat{J}(k-1)) \end{aligned} \tag{21}$$

where $\delta = [1, 0, \ldots, 0]$.

Thus, combining (11), (12), (21), the total control action can be stated as:

$$\begin{aligned} u(k) =& u(k-1) + \frac{\hat{\phi}(k)}{\hat{\phi}^2(k)+\sigma} (\tilde{y}(k+1) - \hat{y}_s(k) \\ & - (2+K_s)e_s(k) + e_s(k-1) - \frac{e^*(k)}{1+\lambda T}) \\ & - \delta(\Gamma^T_\Delta \hat{\Theta}^T \hat{\Theta} \Gamma_\Delta + R_u)^{-1} (\Pi^T \mu^* + \Gamma^T_\Delta \\ & \times (-\hat{\Theta})^T (s(k) + \Upsilon \hat{J}(k-1)) \end{aligned} \tag{22}$$

Remark 3: Sliding mode predictive control is based on the rolling optimization of the data model and the state of the sliding mode surface function, solving the optimization problem in the finite time domain at each sampling moment k. The first element of the solution acts on the control system, making it possible to correct various distortion and error problems effectively and timely in the actual control process.

Remark 4: The control scheme (22) contains input-based feedforward, observation error-based feedforward compensation, and sliding mode state-based feedback compensation with explicit and active handling of control and control increment constraints.

C. STABILITY ANALYSIS

Theorem: The nonlinear system (1) is controlled by the MFASPC scheme (22), and the tracking error converges to the bounded region by $\lim_{k\to\infty}|e^*(k)| \leq \frac{\zeta_1+\sqrt{\zeta^2+4\zeta_0\zeta_2}}{2\zeta_0\lambda T}$, where ζ_0 is given as $\zeta_0 \leq \frac{\hat{\phi}^2(k)(\hat{\phi}^2(k)+\sigma)}{(\hat{\phi}^2(k)+\sigma)^2}$, ζ_1 is defined as:

$$\zeta_1 = \frac{2\sigma^3(1+\lambda T)}{(\hat{\phi}^2(k)+\sigma)^3}j(k) \tag{23}$$

ζ_2 is denoted as:

$$\zeta_2 = (\frac{\sigma^2(1+\lambda T)}{(\hat{\phi}^2(k)+\sigma)^2}j(k))^2 \tag{24}$$

Proof: The MFASPC designed above is based on the data model. The PPD estimates are an essential part of the data model, so analyzing the boundedness of the PPD estimates is imperative. By subtracting (5) from $\phi(k-1)$, the dynamic properties of the PPD estimation error can be obtained:

$$\bar{\phi}(k+1) = (1 - \frac{2\Delta u^2(k)}{\Delta u^2(k)+\chi})\bar{\phi}(k) \tag{25}$$

Consider the Lyapunov function:

$$V_1(k) = \alpha_s e_s^2(k) + \beta_\phi \bar{\phi}^2(k) \tag{26}$$

where $\alpha_s > 0$,β_ϕ. Substituting in (4)(25) to (26), we get:

$$\begin{aligned}\Delta V_1(k+1) &= \alpha_s((1-K_s)^2-1)e_s^2(k) + 2\alpha_s(1-K_s)\\ &\quad\times \Delta u(k)\bar{\phi}(k)e_s(k) - (\frac{4\beta_\phi\chi}{(\Delta u^2(k)+\chi)^2}\\ &\quad-\alpha_s)\Delta u^2(k)\bar{\phi}^2(k)\\ &\leq (\alpha_s((1-K_s)^2-1)+\alpha_s^2)e_s^2(k)\\ &\quad-(\frac{4\beta_\phi\chi}{(\Delta u^2(k)+\chi)^2}-\alpha_s-(1-K_s)^2)\\ &\quad\times\Delta u^2(k)\bar{\phi}^2(k)\end{aligned} \tag{27}$$

where $\alpha_s((1-K_s)^2-1) < 0$. If the appropriate α_s, β_ϕ, χ are chosen such that:

$$\alpha_s((1-K_s)^2-1)+\alpha_s^2 < 0$$
$$\frac{4\beta_\phi\chi}{(\Delta u^2(k)+\chi)^2} - \alpha_s - (1-K_s)^2 > 0$$

Then $\Delta V_1(k+1) \leq 0$, when $k\to\infty$, $\Delta V_1(k)\to 0$. This means that $\lim_{k\to\infty} e_s(k) = 0$ and $\bar{\phi}(k)$ is bounded. Since $\phi(k)$ is bounded, so $\hat{\phi}(k)$ is bounded.

By defining the Lyapunov function as $V_2(k) = s^2(k)$, the variation of the Lyapunov function of the discrete system can be obtained as

$$\Delta V_2(k+1) = s^2(k+1) - s^2(k) \tag{28}$$

For simplicity, assuming no control action and constraint penalty, i.e., $\mu^* = R_u = 0$, the arrival condition of the sliding die surface can be derived as:

$$\begin{aligned}s(k+1)+s(k) &= \frac{\sigma^2(1+\lambda T)}{(\hat{\phi}^2(k)+\sigma)^2}j(k) + \frac{\hat{\phi}^2(k)+2\sigma}{\hat{\phi}^2(k)+\sigma}s(k)\\ s(k+1)-s(k) &= \frac{\sigma^2(1+\lambda T)}{(\hat{\phi}^2(k)+\sigma)^2}j(k) - \frac{\hat{\phi}^2(k)}{\hat{\phi}^2(k)+\sigma}s(k)\end{aligned} \tag{29}$$

Combining (29) and (28), we get:

$$\begin{aligned}\Delta V(k+1) &= -\frac{\hat{\phi}^2(k)(\hat{\phi}^2(k)+\sigma)}{(\hat{\phi}^2(k)+\sigma)^2}s^2(k) + \frac{2\sigma^3(1+\lambda T)}{(\hat{\phi}^2(k)+\sigma)^3}\\ &\quad j(k)s(k) + (\frac{\sigma^2(1+\lambda T)}{(\hat{\phi}^2(k)+\sigma)^2}j(k))^2\\ &\leq -\zeta_0 s^2(k) + \zeta_1 s(k) + \zeta_2\end{aligned} \tag{30}$$

when $s(k) > (\zeta_1 + \sqrt{\zeta_1^2 + 4\zeta_0\zeta_2})/(2\zeta_0)$, there is $\Delta V(k) < 0$, so the sliding mode function s(k) is bounded, that is, there exists $\xi_s = (\zeta_1(k) + \sqrt{\zeta_1^2(k) + 4\zeta_0\zeta_1(k)})/(2\zeta_0)$, such that:

$$\lim_{k\to\infty}|s(k)| \leq \xi_s \tag{31}$$

According to the definition of integral sliding surface (9), the relationship between the sliding surface and the tracking error can be obtained:

$$e^*(k+1) = \frac{e^*(k)}{1+\lambda T} + \frac{s(k+1)-s(k)}{1+\lambda T}$$

Taking absolute values on both sides has:

$$\begin{aligned}|e^*(k+1)| &\leq |\frac{e^*(k)}{1+\lambda T}| + |\frac{s(k+1)}{1+\lambda T}| + |\frac{s(k)}{1+\lambda T}|\\ &\leq |\frac{e^*(1)}{(1+\lambda T)^k}| + |\frac{2\xi_s(1-\frac{1}{(1+\lambda T)^k})}{\lambda T}\end{aligned}$$

Since $\lambda > 0$, $T > 0$, then $0 < \frac{1}{1+\lambda T} < 1$, we can get:

$$\lim_{k\to\infty} e^*(k) = \frac{2\xi_s}{\lambda T} \tag{32}$$

Together with (17), the following result can be introduced:

$$\lim_{k\to\infty}|e^*(k)| \leq \frac{\zeta_1(k) + \sqrt{\zeta_1^2(k) + 4\zeta_0(k)\zeta_2(k)}}{\zeta_0(k)\lambda T} \tag{33}$$

The general idea of the above control scheme is shown in Fig.1. As shown in Fig.1, the execution of the algorithm is divided into five phases: Initialization, Follow up the work point, Equivalent dynamic linearization, Controller design, and Control execution. As indicated by the red arrow, when the fifth step is finished, it is necessary to determine whether the work point is finished, and it will continue with phases two to five until the work point. If not, stages two through five will continue until the end of the work point.

The control block diagram is shown in Fig.2. It can be seen that the whole control scheme consists of two parts, the CFDL stage, and the sliding mode predictive controller stage, respectively. The first stage requires the estimation of PPD and data model using the designed observer. The second

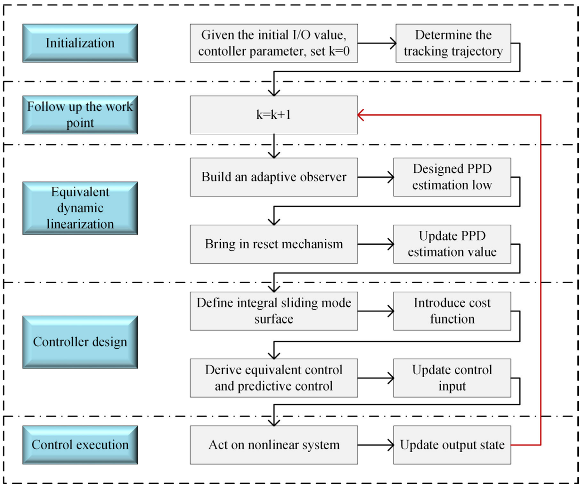

FIGURE 1. **Implementation process of the proposed algorithm.**

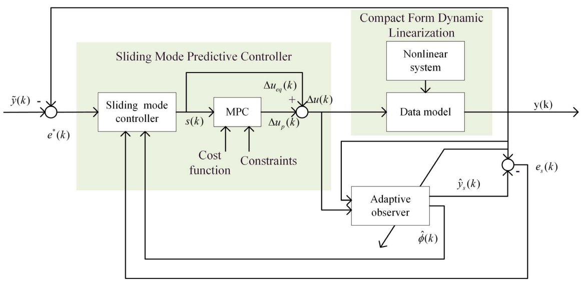

FIGURE 2. **Control block diagram of the proposed algorithm.**

stage is based on the data model established in the previous stage. The model predictive control takes the sliding mode state as input, optimizes the sliding mode state, and combines the equivalent control to form the total control input of the discrete-time nonlinear system.

IV. SIMULATION

In this section, we will conduct two simulation experiments, including numerical simulation in a general sense and PV system simulation. It is worth mentioning that although mathematical models are listed in both experiments, they are only used to generate output and input data, and the controller design does not rely on the listed models.

A. NUMERICAL SIMULATION

The following nonlinear systems exist:

$$y(k+1) = sin(y(k)) + u(k)(5 + cos(y(k)u(k))); \tag{34}$$

The tracking track is set to:

$$\begin{aligned}\tilde{y}(k) \\ &= 1 + 0.2(sin(2k\pi/50) + sin(2k\pi/150) + sin(2k\pi/200))\end{aligned} \tag{35}$$

The working point is set to [0,1000], and the parameters of the proposed controller are set as $u(1) = u(2) = 0$, $y(1) = y(2) = 0$, $K_s = 0.8$, $\sigma = 0.02$, $\chi = 80$, $\lambda = 1.8$, $T = 0.02$, $\hat{\psi}(1) = 13$, $\varsigma = 0.0001$, $N_y = N_u = 12$, $R_u = 0.01$. For comparison with the conventional MFAC and CFDL-DITSMC [28] respectively, the parameters of the conventional MFAC are set as:$\mu = 0.5$, $\eta = 0.3$, $\rho = 0.6$, $\eta = 0.3$; the parameters of CFDL-DITSMC are set as :$\mu = 0.5$, $\eta = 0.3$, $\lambda_s = 0.0002$, $\mu = 0.5$, $\lambda_1 = 0.3$, $\lambda_2 = 025$, $\alpha = 5/7$, $\omega = 0.01$, $\delta = 3$. The simulation results are shown in Figs.3-6, representing, in turn, the output, input, PPD estimation, and error performance of the system (34) under three different control schemes. Among them, the error performance of Fig.6 is the absolute value of the error, which reflects the magnitude of the offset produced between the zero errors. In the simulation, the red dashed line characterizes the performance of the proposed scheme. In contrast, the dark blue dashed line and the light blue solid line indicate the control performance curves under CFDL-DITSMC and MFAC methods. It can be seen that the system can achieve the tracking task of the desired trajectory with the controller MFAC, CFDL-DITSMC, and MFASPC. Nevertheless, they differ slightly in specific tracking details, with MFAC having the most intense transient performance, larger overshoot, larger steady-state error, and large PPD variation. The control effect of CFDL-DITSMC is significantly stronger than the former, as reflected in the output signal, input signal, PPD, and tracking error, but is accompanied by a more pronounced signal oscillation phenomenon, which is related to the switching control term in the traditional sliding mode control, while the MFASPC proposed in this paper shows a better tracking effect, with smaller overshoot and tracking error, good tracking speed and control accuracy.

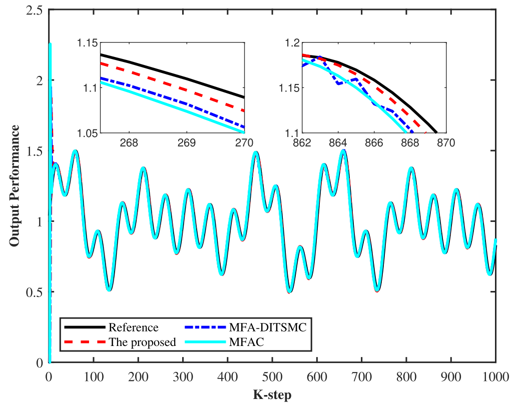

FIGURE 3. **Output performance under different control scheme.**

Select evaluation indicators $MeanSquaredError(MSE)$ and Root Mean Squared Error(RMSE), where $MSE = \frac{1}{N}\sum_{k=1}^{N} e^*(k)^2$ and $RMSE = \sqrt{\frac{1}{N}\sum_{k=1}^{N} e^*(k)^2}$, $N = 1000$, and calculate the MSE and RMSE under the three controllers in the above simulation experiments. As shown in Table 1, it is clear that the proposed MFASPC method has superior tracking performance compared to MFA-DITSMC and MFAC.

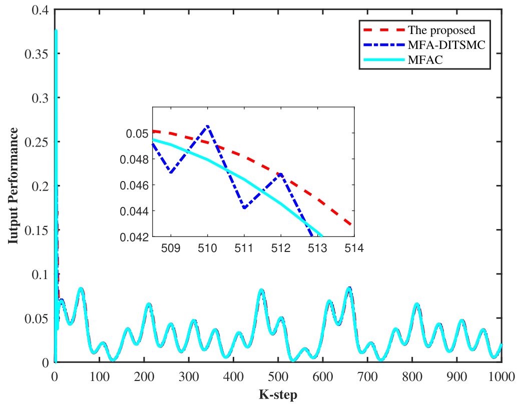

FIGURE 4. Input performance under different control scheme.

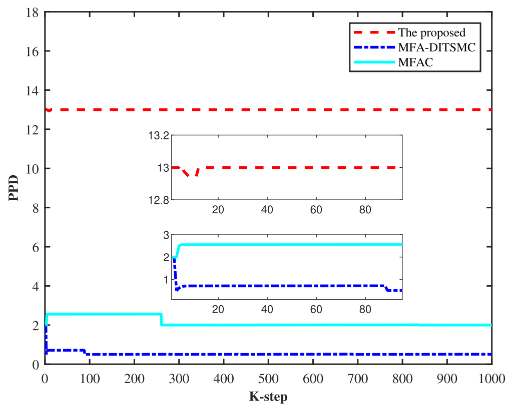

FIGURE 5. PPD estimation under different control scheme.

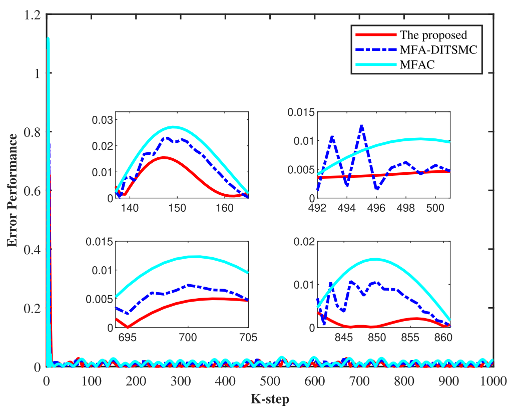

FIGURE 6. Error performance under different control scheme.

TABLE 1. Comparison between three controller.

Metrics	MFASPC	MFA-DITSMC	MFAC
MSE	2.01×10^{-3}	2.79×10^{-3}	3.51×10^{-3}
RMSE	44.8×10^{-3}	52.8×10^{-3}	59.2×10^{-3}

Remark 5: The signal oscillation phenomenon is common in sliding mode control applications. In order to suppress the influence of disturbances, a coefficient more significant than the bounded disturbance will be selected as the switching term in the switching function; that is, based on the worst perturbation given by the estimated value, the flexibility is poor, especially in discrete-time nonlinear systems oscillation phenomenon is more apparent. The proposed method uses the rolling optimization principle to select the first control input of the control sequence generated by each sampling point instead of the original switching control to ensure accurate tracking along the tracking trajectory.

If interference input is added, the new input becomes:

$$u'(k) = u(k) + 0.01sin(2k\pi/20) \tag{36}$$

Again using the above three controllers with constant parameters, the corresponding output performance, input performance, incremental input performance, and error performance are shown in Figs.7-10. It is observed that the performance of the controllers is all affected when there are external disturbance inputs, among which the MFAC with the light blue solid line has the most significant impact, and the CFDL-DITSMC with dark blue dashed line has some ability to suppress the interference. However, the phenomenon of signal oscillation still exists, which is reflected in both output, input, input increment, and error performance. The MFASPC (solid red line) proposed in this paper predicts the optimal control for the next step in advance and uses it for the arrival stage control with some compensation for disturbances, making it better than the previous two controllers in terms of tracking effect.

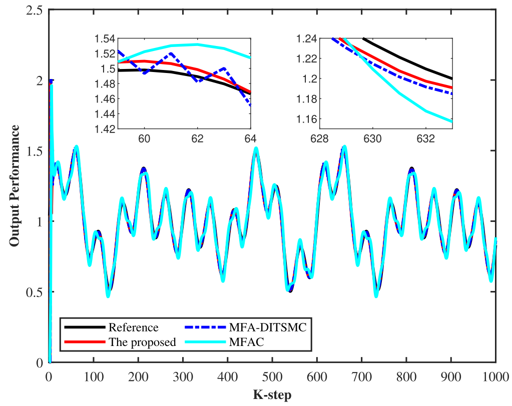

FIGURE 7. Output performance under disturbance.

B. PHOTOVOLTAIC POWER GENERATION SYSTEM

Photovoltaic power generation system is a commonly used device for converting solar energy into electrical energy, which achieves energy conversion through the photovoltaic effect and improves the penetration of clean energy. Photovoltaic modules or photovoltaic arrays composed of photovoltaic cells meet the demand for different power. However, the output characteristics (power-voltage characteristics, current-voltage characteristics) are susceptible to the influence of external temperature, light intensity, and other factors and have strong nonlinearity. Using the PV cell model

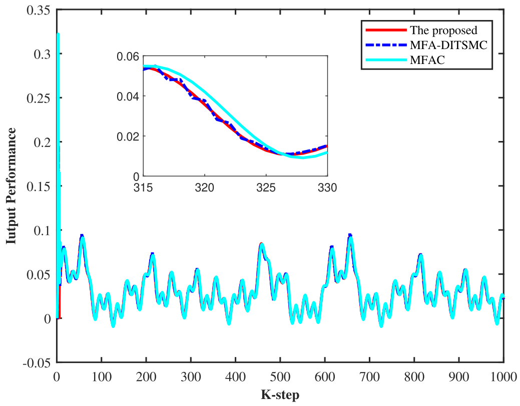

FIGURE 8. Input performance under disturbance.

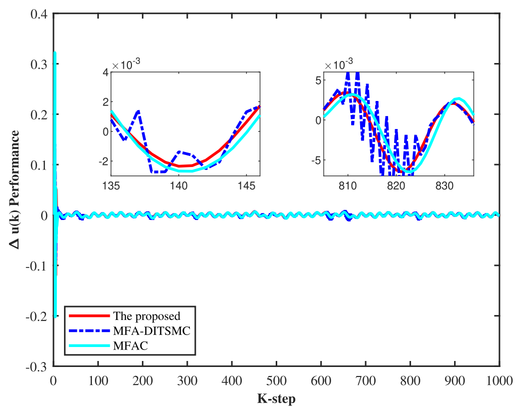

FIGURE 9. Input increment under disturbance.

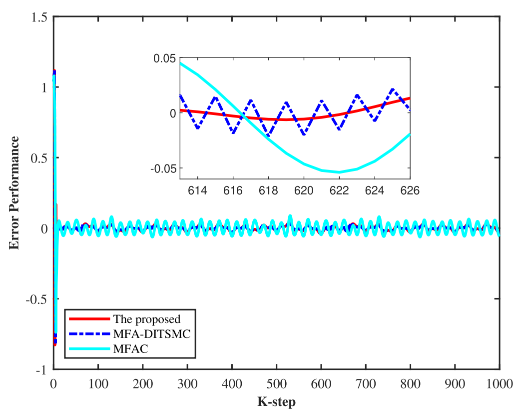

FIGURE 10. Error performance under disturbance.

from the literature [30].

$$\begin{cases} I = I_{pv} - I_d[exp(\frac{U + (n_s/n_p)IR_s}{n_s W}) - 1] - \frac{U + (n_s/n_p)IR_s}{(n_s/n_p)R_p} \\ I_{pv} = n_p(I_{sc\_STC} + k_i \Delta T)\frac{S}{S_{STC}} \\ I_d = n_p \frac{I_{sc\_STC} + k_i \Delta T}{exp(\frac{n_s(U_{oc\_STC} + k_v \Delta T)}{n_s U_T}) - 1]} \end{cases} \tag{37}$$

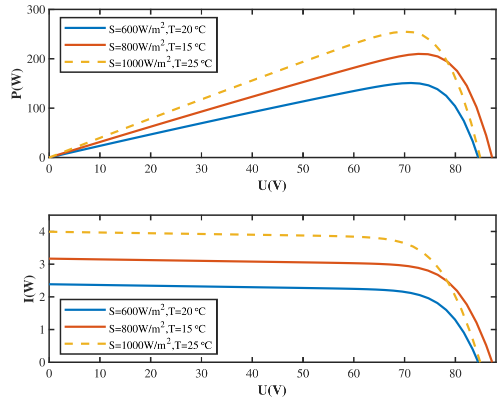

FIGURE 11. PV output characteristic curve.

where I and U are the PV cell output current and voltage, I_{pv} and I_d represent the photogenerated current, and parallel diode current, R_p, R_s, n_p and n_s denote the resistance values of the parallel and series resistors and the corresponding numbers, respectively. Let the temperature and light amplitude under standard test conditions be defined as $T = 25°C, S = 1000W/m^2$, then parameters with suffix STC such as S_{STC} denote standard light $1000W/m^2$. At the same time, I_{sc_STC}, U_{oc_STC} refer to the short-circuit current and open-circuit voltage under standard conditions, $W = \frac{aKT}{q}$, are defined by electron charge q, Boltzmann constant K, temperature T, and diode ideality factor a, k_i,k_v are the current temperature coefficient and voltage temperature coefficient. The specific parameter values are the same as in the literature [30].

Usually, under the same light and temperature conditions, the output power will peak with the voltage increase, which we call the maximum power point. Once the external conditions change, the maximum power point will also change, exhibiting a robust non-linear characteristic. Take three different irradiances and temperatures, for example, the standard condition $S = 1000W/m^2$, $T = 25°C$ and the non-standard condition I $S = 800W/m^2$, $T = 15°C$, the non-standard condition II $S = 600W/m^2$, $T = 20°C$, their output characteristics are shown in Fig.11, where the dashed line indicates the standard condition, and the solid red line and solid blue line characterize the non-standard conditions I and II, respectively. The upper half represents the power versus voltage curve, and the lower half represents the current versus voltage curve. It is clear that each condition has one and only one maximum power point and is different from each other. Solar power will be fully utilized if the PV array always operates at the maximum power point. However, the continuous temperature or light amplitude changes make tracking the maximum power point very difficult. In order to make the PV array always work at the maximum power point, this paper uses the input and output data generated by the PV cell model(37), adjusts the on/off of the insulated gate bipolar transistor by changing the duty cycle of the input signal of the boost chopper circuit, and uses the sum of the instantaneous rates of change of conductance and conductivity as the output signal

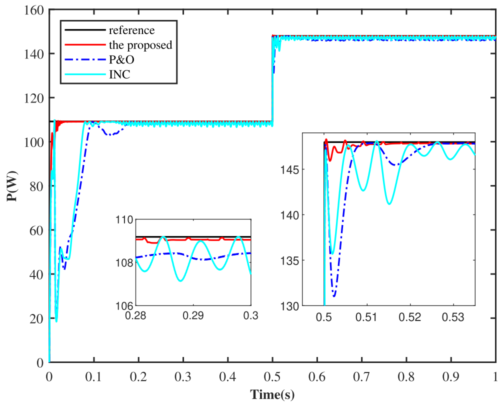

FIGURE 12. **Output power under different control scheme.**

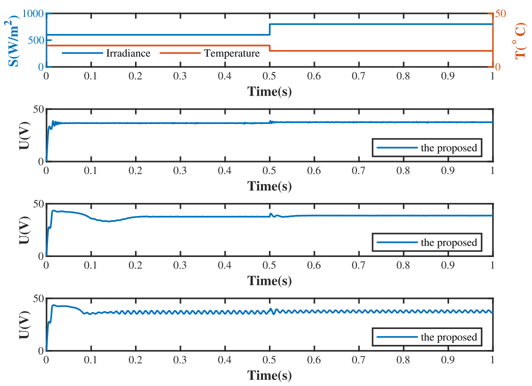

FIGURE 13. **Voltage characteristics under different control scheme.**

to construct an observer-based data-driven model-free sliding mode predictive controller to realize the maximum power point is tracked in real-time. The parameters of the proposed control scheme are set as $K_s = 0.8$, $T = 1e-6$, $\hat{\psi}(1) = 0.02$, $\sigma = 0.02$, $\chi = 80$, $\lambda = 1.8$, $\varsigma = 0.0001$, $N_y = N_u = 12$, $R_u = 0.01$. To verify the validity of the proposed, the traditional maximum power point tracking method of perturbation observation (P&O) [31] and conductivity increment method (INC) [32] are introduced for comparative analysis.

The output power, voltage, and current characteristic curves are shown in Figs.12-14 using three maximum power point tracking methods under the same external light and temperature variation conditions. In Fig.12, when the external environment is under the non-standard condition I, the proposed method represented by the solid red line can track the maximum power point quickly, accompanied by the minor power loss, and the INC method represented by the light blue solid line is slightly better than the P&O method represented by the dark blue dotted line in terms of tracking speed, but the INC method has more oscillations near the maximum power point, and The accuracy is poor. When the external environment changes to non-standard condition II, the maximum power point changes according to the output characteristics of the PV cell. All three methods can track the maximum power point, but the proposed method completes the tracking task

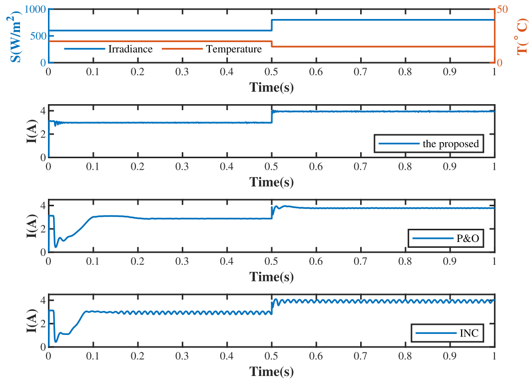

FIGURE 14. **Current characteristics under different control scheme.**

first and avoids unnecessary power waste. At the same time, P&O and INC affect the tracking speed and accuracy because they have to compare the sampled data constantly. The same tracking advantage is reflected in Fig.13 and Fig.14.

V. CONCLUSION

This paper proposes a data-driven model-free adaptive sliding mode predictive control strategy for discrete-time nonlinear systems based on the adaptive observer. This approach relies on adaptive observers to estimate PPD and output, then builds a compact form data model related only to the input and output data. Based on this, rolling optimization is integrated throughout the design of the discrete integral sliding-mode controller to form a novel data-driven sliding-mode predictive controller, which is theoretically verified to be consistently stable in the Lyapunov sense, and the superior tracking control capability is verified through numerical simulations and PV system simulations.

Compared with existing studies, the proposed method is simple, flexible, dynamically updated, and has few design parameters, which is a novel exploration in the framework of observer-based model-free adaptive control theory. In the future, we will carry out research in terms of how to reduce the computational burden.

CONFLICT OF INTEREST STATEMENT

The authors declare that the research was conducted in the absence of any commercial or financial relationships that could be construed as a potential conflict of interest.

REFERENCES

[1] H. Pan, W. Sun, H. Gao, and X. Jing, "Disturbance observer-based adaptive tracking control with actuator saturation and its application," *IEEE Trans. Autom. Sci. Eng.*, vol. 13, no. 2, pp. 868–875, Apr. 2016.

[2] Y. K. Al-Nadawi, X. Tan, and H. K. Khalil, "Inversion-free hysteresis compensation via adaptive conditional servomechanism with application to nanopositioning control," *IEEE Trans. Control Syst. Technol.*, vol. 29, no. 5, pp. 1922–1935, Sep. 2021.

[3] J. G. Stoddard, G. Birpoutsoukis, J. Lataire, and J. S. Welsh, "Frequency domain response under arbitrary excitation for fading memory nonlinear systems," *Automatica*, vol. 107, pp. 327–332, Sep. 2019.

[4] H. Pan and W. Sun, "Nonlinear output feedback finite-time control for vehicle active suspension systems," *IEEE Trans. Ind. Informat.*, vol. 15, no. 4, pp. 2073–2082, Apr. 2019.

[5] Z. Hou and S. Jin, "A novel data-driven control approach for a class of discrete-time nonlinear systems," *IEEE Trans. Control Syst. Technol.*, vol. 19, no. 6, pp. 1549–1558, Nov. 2011.
[6] S. A. Hashjin, A. Corne, S. Pang, K. Ait-Abderrahim, E. Miliani, and B. Nahid-Mobarakeh, "Current sensorless control for WRSM using model-free adaptive control," *IEEE Trans. Transport. Electrific.*, vol. 7, no. 2, pp. 683–693, Jun. 2021.
[7] D. Li and Z. Hou, "Perimeter control of urban traffic networks based on model-free adaptive control," *IEEE Trans. Intell. Transp. Syst.*, vol. 22, no. 10, pp. 6460–6472, Oct. 2021.
[8] Y. Liao, Q. Jiang, T. Du, and W. Jiang, "Redefined output model-free adaptive control method and unmanned surface vehicle heading control," *IEEE J. Ocean. Eng.*, vol. 45, no. 3, pp. 714–723, Jul. 2020.
[9] Y. Hu, Y. Geng, B. Wu, and D. Wang, "Model-free prescribed performance control for spacecraft attitude tracking," *IEEE Trans. Control Syst. Technol.*, vol. 29, no. 1, pp. 165–179, Jan. 2021.
[10] X. Zhong, H. He, D. Wang, and Z. Ni, "Model-free adaptive control for unknown nonlinear zero-sum differential game," *IEEE Trans. Cybern.*, vol. 48, no. 5, pp. 1633–1646, May 2018.
[11] D. Xu, Y. Shi, and Z. Ji, "Model-free adaptive discrete-time integral sliding-mode-constrained-control for autonomous 4WMV parking systems," *IEEE Trans. Ind. Electron.*, vol. 65, no. 1, pp. 834–843, Jan. 2018.
[12] A. M. O. Abbaker, H. Wang, and Y. Tian, "Enhanced model-free discrete-time adaptive terminal sliding-mode control for SOFC power plant with input constraints," *Arabian J. Sci. Eng.*, vol. 47, pp. 1–14, Jul. 2022.
[13] D. Liu and G. Yang, "Prescribed performance model-free adaptive integral sliding mode control for discrete-time nonlinear systems," *IEEE Trans. Neural Netw. Learn. Syst.*, vol. 30, no. 7, pp. 2222–2230, Jul. 2019.
[14] M. Liu, Z. Zhao, and L. Hao, "Data-driven sliding mode control of shape memory alloy actuators with prescribed performance," *Smart Mater. Struct.*, vol. 30, no. 6, Jun. 2021, Art. no. 065012.
[15] W. Zhang, D. Xu, B. Jiang, and T. Pan, "Prescribed performance based model-free adaptive sliding mode constrained control for a class of nonlinear systems," *Inf. Sci.*, vol. 544, pp. 97–116, Jan. 2021.
[16] X. Wang, X. Li, J. Wang, X. Fang, and X. Zhu, "Data-driven model-free adaptive sliding mode control for the multi degree-of-freedom robotic exoskeleton," *Inf. Sci.*, vol. 327, pp. 246–257, Jan. 2016.
[17] S. Han, H. Wang, and Y. Tian, "Model-free based adaptive nonsingular fast terminal sliding mode control with time-delay estimation for a 12 DOF multi-functional lower limb exoskeleton," *Adv. Eng. Softw.*, vol. 119, pp. 38–47, May 2018.
[18] R.-E. Precup, M.-B. Radac, R.-C. Roman, and E. M. Petriu, "Model-free sliding mode control of nonlinear systems: Algorithms and experiments," *Inf. Sci.*, vol. 381, pp. 176–192, Mar. 2017.
[19] B. Esmaeili, M. Salim, and M. Baradarannia, "Predefined performance-based model-free adaptive fractional-order fast terminal sliding-mode control of MIMO nonlinear systems," *ISA Trans.*, vol. 131, pp. 108–123, Dec. 2022.
[20] Y. Chen, C. Tang, and M. Roohi, "Design of a model-free adaptive sliding mode control to synchronize chaotic fractional-order systems with input saturation: An application in secure communications," *J. Franklin Inst.*, vol. 358, no. 16, pp. 8109–8137, Oct. 2021.
[21] H. Gao, G. Ma, Y. Lv, and Y. Guo, "Forecasting-based data-driven model-free adaptive sliding mode attitude control of combined spacecraft," *Aerosp. Sci. Technol.*, vol. 86, pp. 364–374, Mar. 2019.
[22] Q. Xu, "Digital integral terminal sliding mode predictive control of piezoelectric-driven motion system," *IEEE Trans. Ind. Electron.*, vol. 63, no. 6, pp. 3976–3984, Jun. 2016.
[23] L. He, F. Wang, and D. Ke, "FPGA-based sliding-mode predictive control for PMSM speed regulation system using an adaptive ultralocal model," *IEEE Trans. Power Electron.*, vol. 36, no. 5, pp. 5784–5793, May 2021.
[24] X. Li, G. Sun, and X. Shao, "Discrete-time pure-tension sliding mode predictive control for the deployment of space tethered satellite with input saturation," *Acta Astronautica*, vol. 170, pp. 521–529, May 2020.
[25] H. Li, L. Bi, and J. Yi, "Sliding-mode nonlinear predictive control of brain-controlled mobile robots," *IEEE Trans. Cybern.*, vol. 52, no. 6, pp. 5419–5431, Jun. 2022.
[26] S. Kang, H. Wu, X. Yang, Y. Li, J. Yao, B. Chen, and H. Lu, "Discrete-time predictive sliding mode control for a constrained parallel micropositioning piezostage," *IEEE Trans. Syst., Man, Cybern. Syst.*, vol. 52, no. 5, pp. 3025–3036, May 2022.
[27] M. S. Mousavi, S. A. Davari, V. Nekoukar, C. Garcia, and J. Rodriguez, "Model-free predictive control based on the integral sliding mode observer for induction motor," in *Proc. 13th Power Electron., Drive Syst., Technol. Conf. (PEDSTC)*, Feb. 2022, pp. 113–117.
[28] Y. Wang and M. Hou, "Model-free adaptive integral terminal sliding mode predictive control for a class of discrete-time nonlinear systems," *ISA Trans.*, vol. 93, pp. 209–217, Oct. 2019.
[29] J. Zhang, S. Chai, B. Zhang, and G. Liu, "Distributed model-free sliding-mode predictive control of discrete-time second-order nonlinear multiagent systems with delays," *IEEE Trans. Cybern.*, vol. 52, no. 11, pp. 12403–12413, Nov. 2022.
[30] K. Ishaque, Z. Salam, and H. Taheri, "Simple, fast and accurate two-diode model for photovoltaic modules," *Sol. Energy Mater. Sol. Cells*, vol. 95, no. 2, pp. 586–594, Feb. 2011.
[31] M. F. N. Tajuddin, M. S. Arif, S. M. Ayob, and Z. Salam, "Perturbative methods for maximum power point tracking (MPPT) of photovoltaic (PV) systems: A review," *Int. J. Energy Res.*, vol. 39, no. 9, pp. 1153–1178, Jul. 2015.
[32] K. S. Tey and S. Mekhilef, "Modified incremental conductance MPPT algorithm to mitigate inaccurate responses under fast-changing solar irradiation level," *Sol. Energy*, vol. 101, pp. 333–342, Mar. 2014.

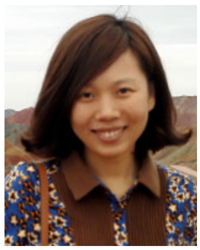

BING REN was born in China. She received the M.S. degree in control theory and control engineering from the Lanzhou University of Technology, Lanzhou, China, where she is currently pursuing the Ph.D. degree with the School of Automation and Electrical Engineering. Her current research interests include data-driven control and adaptive control.

GUANGQING BAO was born in China. She received the Ph.D. degree from Shanghai University. She is currently a professor and a doctoral supervisor. She is also a Special Professor of "Flying Scholar" of Gansu Province, selected as "555 Science and Technology Talent Project," Gansu Province Leading Talents, Gansu Province Long Yuan Innovative Talents, and Gansu Province Outstanding Youth Fund Candidate, the Head of the Gansu Province University Collaborative Innovation Team, a Visiting Scholar with The University of Manchester, U.K., a Visiting Scholar of "Western Light," and a Visiting Scholar with the Institute of Electrical Engineering, Chinese Academy of Sciences. Her research interests include modern electrical machinery and measurement and control technology, new energy generation and grid control, and power system intelligent planning.